# Single crystal coordinating solvent exchange as a general method for the enhancement of the photoluminescence properties of lanthanide MOFs

**Article** *in* Journal of Materials Chemistry A · January 2014

DOI: 10.1039/C3TA14489E

CITATIONS
31

READS
190

**7 authors**, including:

Theodore Lazarides
Aristotle University of Thessaloniki
**52** PUBLICATIONS **2,433** CITATIONS

SEE PROFILE

Spyridon Kaziannis
University of Ioannina
**33** PUBLICATIONS **360** CITATIONS

SEE PROFILE

C. Kosmidis
University of Ioannina
**138** PUBLICATIONS **1,967** CITATIONS

SEE PROFILE

G. Itskos
University of Cyprus
**78** PUBLICATIONS **2,328** CITATIONS

SEE PROFILE

Journal of Materials Chemistry A

PAPER

# Single crystal coordinating solvent exchange as a general method for the enhancement of the photoluminescence properties of lanthanide MOFs†

Cite this: *J. Mater. Chem. A*, 2014, **2**, 5258

Eleni J. Kyprianidou,[a] Theodore Lazarides,[b] Spyridon Kaziannis,[c] Constantine Kosmidis,[c] Grigorios Itskos,[d] Manolis J. Manos*[b] and Anastasios J. Tasiopoulos*[a]

Received 2nd November 2013
Accepted 17th January 2014

DOI: 10.1039/c3ta14489e

www.rsc.org/MaterialsA

The discovery of new methods for the post-synthesis modification of materials is essential in order to establish suitable strategies for the tuning of their properties in a rational manner. Here we present a series of single-crystal-to-single-crystal (SCSC) transformations for the flexible $[Eu_2(ClP)_2(DMF)_2(H_2O)_2]$ (**UCY-8**) [$H_3ClP$ = 5-(4-carboxybenzylideneamino)isophthalic acid] and rigid $[Eu_2(N\text{-}BDC)_3(DMF)_4]$ (**EuN-BDC**) ($H_2N$-BDC = 2-amino-1,4-benzene dicarboxylic acid) Metal–Organic Frameworks (MOFs) that involve the replacement of their coordinating solvent molecules by terminally ligating organic molecules with multiple functional groups including –OH, –SH, –NH– and $–NH_2$ or their combinations, chelating ligands, and two different organic compounds. The capability of the flexible MOF, which contains small pores and channels (<4 Å), to exchange its coordinating solvent molecules by relatively bulky molecules (such as pyridine, 2-hydroxymethyl-phenol, *etc.*) is shown to be the result of its breathing capacity. Remarkably, the rigid MOF is also highly capable of replacing its coordinating solvent molecules by bulky ligands, despite its small pores (2–5 Å) and lack of structural flexibility. Interestingly, the insertion of some organic ligands into the rigid MOF results in a significant modification of its framework structure and substantial expansion of its potential void space. Not only a plethora of exchanged analogues of these MOFs have been isolated and crystallographically characterized, but also, in some cases, a tremendous enhancement of their $Eu^{3+}$-based photoluminescence (PL) signals, lifetimes and quantum yields (up to ~16 times) compared to those of the pristine materials has been observed due to the replacement of terminal solvents by organic ligands being efficient sensitizers for the $Eu^{3+}$ ion. Overall this work indicates that the Single Crystal Coordinating Solvent Exchange (SCCSE) can be applied as a general post-synthetic modification method for LnMOFs and also constitutes a highly efficient strategy for the enhancement of the $Ln^{3+}$-based PL.

## Introduction

Metal–organic frameworks (MOFs) have attracted a tremendous amount of attention not only because of their unique structures and topologies,[1,2] but also due to their significance in various technological and scientific fields such as gas storage and separation,[3–6] magnetism,[7] sensing,[8] drug delivery[9] and catalysis.[10] Although a large variety of MOFs have been reported, it remains challenging to modify and tune their properties in a rational manner. To this end, many research groups are now focusing on the development of efficient methods for the post-synthetic modification (PSM) of MOFs.[11–13] It is preferable that such post-synthetic modifications proceed in a single-crystal-to-single-crystal (SCSC) fashion in order to gain direct and accurate structural information for the modified compounds. Such SCSC modifications involve mainly three different types of structural alterations: (a) insertion/removal of guest molecules,[13–15] (b) modifications of the organic ligands[11,16–18] and (c) changes in the coordination environment of metal ions.[11,13a,19,20,21] However, SCSC transformations of types (b) and

[a]*Department of Chemistry, University of Cyprus, 1678 Nicosia, Cyprus. E-mail: atasio@ucy.ac.cy; Fax: +357-22-895451; Tel: +357-22-892765*

[b]*Department of Chemistry, University of Ioannina, 45110, Ioannina, Greece. E-mail: emanos@cc.uoi.gr*

[c]*University of Ioannina Laser facility, Department of Physics, University of Ioannina, Ioannina 45110, Greece*

[d]*Department of Physics, University of Cyprus, 1678 Nicosia, Cyprus*

† Electronic supplementary information (ESI) available: Elemental analysis data, structural figures, selected FT-IR spectra, experimental details and single crystal X-ray crystallographic data for all new compounds. CCDC 941883–941909. For ESI and crystallographic data in CIF or other electronic format see DOI: 10.1039/c3ta14489e

(c) are rarely observed because they result in the break of covalent or coordination bonds and formation of new ones that usually deteriorate the long-range structural order of the pristine compounds. $Ln^{3+}$ MOFs (LnMOFs) with polycarboxylate ligands seem to be excellent candidates for studying SCSC transformations of type (c), because they possess high stability in air and weakly bound solvent ligands that could be easily removed without collapse of their frameworks.[21,22] Thus, we have recently began to investigate the synthesis of new LnMOFs and the study of their SCSC coordinating solvent exchange properties. The first result of these studies included the isolation of a flexible $Nd^{3+}$ MOF $[Nd_2(CIP)_2(DMF)_{2.8}(H_2O)_{1.2}]$ (**UCY-2**), based on the semi-rigid tricarboxylic ligand $H_3CIP$ [$H_3CIP$ = 5-(4-carboxybenzylideneamino)isophthalic acid], which showed an extraordinary capability to undergo a series of SCSC transformations.[21] The latter involved the exchange of the coordinating solvent molecules of **UCY-2** by various terminal and chelating ligands as well as anions and combinations of organic molecules. These SCSC modifications were not only highly unusual but also resulted in the insertion into the structure of **UCY-2** of various unbound functional groups, including functionalities such as –SH that have not been incorporated previously into MOFs.[21] Furthermore, we have recently demonstrated the usefulness of the coordinating solvent exchange capability of **UCY-5** (the $Ce^{3+}$ analogue of **UCY-2**) for the selective sorption of MeOH in the liquid phase.[23]

As an expansion of this work, our research efforts are now focused on the establishment of the Single Crystal Coordinating Solvent Exchange (SCCSE) as a generally applied strategy for the incorporation of functional groups into the structures of LnMOFs. In addition, we aim to utilize this method for the targeted modification or/and improvement of the properties of these MOFs. A property of LnMOFs that could be enhanced by applying the SCCSE strategy is their $Ln^{3+}$-based photoluminescence (PL), which is known to be sensitive to the coordination environment of the lanthanide ion.[22] The establishment of a facile and highly efficient method to improve the PL of LnMOFs is of significant importance because it can lead to the development of superior photoluminescent materials. Such materials would be particularly attractive for various applications related to lighting, sensing, optical devices, photocatalysis and photon harvesting in photovoltaic technology.[22]

We herein describe a plethora of SCSC solvent exchange transformations for two different types of LnMOFs, the flexible $[Eu_2(CIP)_2(DMF)_2(H_2O)_2]$ (**UCY-8**) (ref. 23) and the rigid $[Eu_2(N\text{-}BDC)_3(DMF)_4]$ (**EuN-BDC**) (N-BDC = 2-amino-1,4-benzene dicarboxylate).[24] These modifications comprise the exchange of the coordinating and/or guest solvent molecules of **UCY-8** and **EuN-BDC** by (i) terminal ligands with multiple functional groups (including among others relatively bulky organic molecules such as 2-hydroxy-phenol and benzimidazole), (ii) chelating organic ligands (imidazole or pyridine analogues), (iii) two different terminal ligands and (iv) various organic compounds – guest molecules. The SCCSE is thus shown to be applicable for the post-synthesis modification of LnMOFs with substantially different structural characteristics. In addition, the PL properties of the various exchanged materials were investigated in detail indicating in some cases a huge amplification of the $Eu^{3+}$ emission signals, lifetimes and quantum yields compared to those of the as-prepared MOFs. Thus, SCCSE is demonstrated as a general method for the targeted modification of the structures of LnMOFs and the enhancement of their PL properties.

## Results and discussion

### SCSC transformations for UCY-8 and EuN-BDC

The presence of highly disordered coordinating solvent molecules in **UCY-8** and **Eu-NBDC** in combination with their relatively open structure and excellent stability in air (for several months) and various solvents (including water) prompted us to investigate the SCSC solvent exchange properties of these compounds. We have chosen flexible (**UCY-8**) and rigid (**EuN-BDC**) MOFs to check whether it is possible to apply the SCSC coordinating solvent exchange method for various LnMOFs independently of their structural characteristics. We have focused on $Eu^{3+}$ MOFs for these studies, as one of our main targets was to investigate the effect of the incorporation of various organic ligands on the $Eu^{3+}$-based PL properties of these materials.

**UCY-8**, recently reported by our group,[23] crystallizes in the monoclinic space group $C2/c$ and contains the dinuclear building block $[Eu_2(COO)_6(DMF)_2(H_2O)_2]$ [Fig. S1 in the ESI†] as the secondary building unit (SBU). The compound displays a three-dimensional structure (Fig. S2†) with a topology corresponding to that of flu-3,6-$C2/c$ nets and narrow channels (3–4 Å).[21,23] **UCY-8**, which is based on the semi-rigid tricarboxylic ligand $H_3CIP$, is expected to present significant structural flexibility that may result in highly unusual SCSC transformations as observed in the case of its analogue **UCY-2**.[21]

**EuN-BDC**, reported by Reedijk *et al.*,[24] crystallizes in the triclinic space group $P\bar{1}$ and is based on the rigid dicarboxylic ligand N-BDC and dinuclear SBU $[Eu_2(COO)_6(DMF)_4]$. **EuN-BDC** displays a 3D-structure with a $4^{12}\cdot6^3$ topology (Fig. S3†) and small pores (2–5 Å). Taking into account the narrow channels of **EuN-BDC** that theoretically cannot allow the diffusion of bulky organic molecules and its lack of structural flexibility, it would be challenging to investigate whether SCSC coordinating solvent exchange is feasible with such a compound.

Heterogeneous solvent-exchange reactions of single crystals of **UCY-8** or **EuN-BDC** with the organic molecules at 50 °C resulted in single crystals that were macroscopically very similar in size and shape to those of the pristine compounds (Fig. S4 and S5†). The solvent exchange reactions involving liquid organic molecules were performed by immersing single crystals of the MOFs into these liquids followed by the thermal treatment of the mixtures at 50 °C. When, however, the organic ligands were solids, their incorporation into the framework of the MOFs was attempted *via* a solvent-exchange reaction of single crystals of **UCY-8** with a solution of the corresponding organic molecule in a non-coordinating solvent (*e.g.* $CHCl_3$ and $CH_3NO_2$) at 50 °C. All these processes were proven to be SCSC transformations by the determination of the crystal structures of the exchanged compounds. Selected crystal data for

**UCY-8**/**EuN-BDC** and the exchanged analogues are given in Tables S1–S6.† All compounds crystallize in the same space group as the pristine materials with the exception of **UCY-8**/py (see below). The retention of the crystallinity of these materials is reflected by the very good refinement of their crystal structures (all reported $R_1$ values are <8.2%, see Tables S1–S6†). Note, that in all cases several single crystals were examined and found to have identical unit cell parameters. Besides single crystal X-ray crystallography, infrared spectroscopy (IR) also confirmed the replacement of DMF solvent molecules (Fig. S6 and S7†).

A series of SCSC solvent exchange reactions have been performed with imidazole (Im), various analogues of Im, and 3-amino-1*H*-1,2,4-triazole (atzH), since such ligands have been proved efficient sensitizers for $Eu^{3+}$.[25] Furthermore, their insertion into the structure of the MOF as terminal ligands can result in functionalized MOFs with free –NH–, –N═, $–NH_2$ or combinations of these groups.[21]

Thus, the reaction of **UCY-8** with Im afforded a compound containing 2 Im terminal ligands per $Eu^{3+}$ ion (Fig. 1). The experiments with 2-methyl-1*H*-imidazole (2mIm), 4(5)-methyl-1*H*-imidazole (4(5)mIm), 2-ethyl-5-methyl-1*H*-imidazole (etmIm) and atzH yielded products with one Im derivative or atzH and one solvent terminal ligand per $Eu^{3+}$ ion (Fig. 1). The solvent terminal ligands were $H_2O$ (**UCY-8**/4(5)mIm), DMF (**UCY-8**/2mIm, **UCY-8**/atzH) or EtOH (**UCY-8**/etmIm). The latter was not included in the reaction mixture but we speculate that it comes from a partial decomposition of etmIm occurring under the reaction conditions. The guests in these compounds are water molecules; however, **UCY-8**/4(5)mIm contains also uncoordinated 4(5)mIm in its pores.

Reactions were also performed with organic molecules that can act as chelating ligands, namely 1*H*-imidazole-4-carbaldehyde (Ima), 5-methyl-1*H*-imidazole-4-carbaldehyde (mIma) and 2-hydroxymethyl-pyridine (2hmp). Our intention was to replace the two terminal ligands with one chelating ligand for each $Eu^{3+}$, something that could enhance the $Eu^{3+}$ PL signals (*vide infra*). Indeed, in the compounds isolated from the SCSC solvent exchange experiments, the terminal solvent ligands were substituted by chelating Ima, mIma (coordinated through their nitrogen and aldehydic oxygen atoms) or 2hmp (coordinated through its pyridine N and hydroxylic O atoms), Fig. 2.

Solvent exchange reactions have also been carried out with various other aromatic organic ligands, such as 2-hydroxymethyl-phenol ($2hpH_2$), benzimidazole (bzIm), pyridine (py) and its analogue 2-methylpyridine (2mpy). The determination of the crystal structures of these compounds indicated that only $2hpH_2$ and py were inserted as terminal ligands for the $Eu^{3+}$ ions, and specifically **UCY-8**/$2hpH_2$ and **UCY-8**/py contain one $2hpH_2$/one DMF and one py/one $H_2O$ terminal ligand per $Eu^{3+}$ ion respectively (Fig. S8†). **UCY-8**/py includes also 3 py guest molecules (per formula unit) in its pores (Fig. S9†) and crystallizes in the triclinic space group, $P\bar{1}$ as also observed for **UCY-2**/py.[21] The other organic molecules bzIm and 2mpy could not be incorporated as ligands into the crystal structures of the exchanged compounds, but only as guests in their pores interacting through H-bonds with the terminal solvent (DMF and $H_2O$) ligands or carboxylate O atoms (Fig. S10 and S11†).

We have also carried out SCSC solvent exchange experiments with combinations of organic ligands, such as Im and atzH. Thus, the reaction of single crystals of **UCY-8** with an equimolar mixture of Im and atzH in $CHCl_3$ afforded **UCY-8**/Im-atzH, which contains an imidazole and water terminal ligands per $Eu^{3+}$ ion as well as a guest atzH molecule forming relatively strong hydrogen bonds (~2.8 Å) with the terminal water ligand (Fig. S8†). Finally, SCSC exchange reaction was performed with 3-mercapto-1,2-propanediol ($merpdH_2$) to check whether it is possible to isolate a compound with free OH/SH groups, as achieved for **UCY-2**.[21] Indeed the elucidation of the crystal structure of the exchanged compound **UCY-8**/$merpdH_2$ revealed the existence of one $merpdH_2$ and one DMF terminal ligand per $Eu^{3+}$ ion (Fig. S8†). The $merpdH_2$ ligand is coordinated through its one OH, thus leaving free OH and SH groups.

SCCSE reactions with the same organic molecules were also performed with **EuN-BDC**. The Im-exchanged **EuN-BDC**

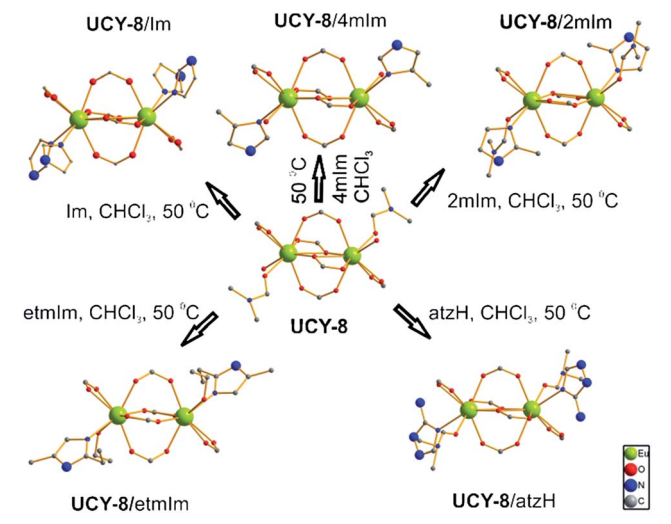


Fig. 1 SCSC transformations that resulted in the exchange of terminal solvent ligands of **UCY-8** by Im, 4(5)mIm, 2mIm, etmIm and atzH; only the SBUs of the pristine and the exchanged products (excluding H atoms) are shown for clarity. For emphasis, the free functional groups are depicted as large balls.

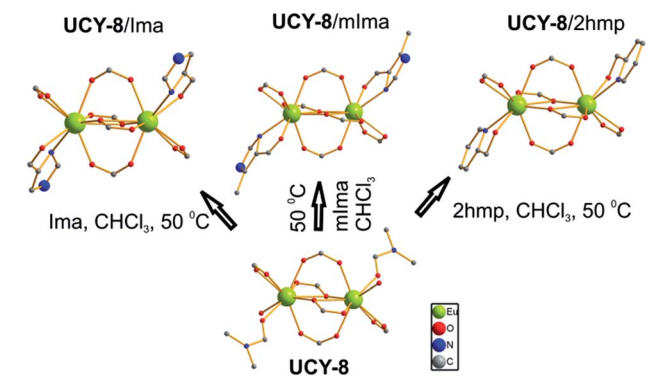


Fig. 2 SCSC transformations that resulted in the exchange of ligated solvent molecules of **UCY-8** by the chelating ligands Ima, mIma and 2hmp.

(**EuN-BDC**/Im) contains two Im molecules terminally coordinated per $Eu^{3+}$ ion, whereas the exchanged compounds with the analogues of Im [2mIm, 4(5)mIm and 5-hydroxymethyl-1*H*-imidazole (hmIm)] include one 2mIm, 4(5)mIm or hmIm and one DMF terminal ligands per $Eu^{3+}$ ion (Fig. 3). Note that it was not possible to isolate an exchanged **EuN-BDC** compound with etmIm, although etmIm can be inserted into the structure of **UCY-8**. However, we were able to synthesize an exchanged analogue of **EuN-BDC** with hmIm, whereas the corresponding analogue of **UCY-8** could not be characterized (due to the poor diffraction quality of its crystals).

It was also possible to insert a number of other terminal ligands into **EuN-BDC**, such as atzH, bzIm, $2hpH_2$, py and 2mpy. Only one of such ligands is inserted per $Eu^{3+}$ ion (or 0.5 2mpy ligands in **EuN-BDC**/2mpy), with the second terminal ligand being DMF, mixed DMF–$H_2O$ or $H_2O$ (Fig. 4). Note that **EuN-BDC**/bzim and **EuN-BDC**/2mpy contain the relatively bulky bzIm and 2mpy as terminal ligands, whereas **UCY-8**/bzim and **UCY-8**/2mpy incorporate these organic molecules as guests. In addition, **EuN-BDC**/py contains py molecules only as ligands, whereas in **UCY-8**/py there are py ligands and py guests as well.

We have also isolated exchanged materials with chelating ligands instead of the terminal ones. Specifically, **EuN-BDC**/Ima and **EuN-BDC**/mIma include a chelating (through imidazole N and aldehydic O) Ima or mIma ligand in place of two DMF terminal ligands per $Eu^{3+}$ ion (Fig. 5). The result of the exchange of single crystals of **EuN-BDC** with 2hmp was quite surprising. The two terminal DMF ligands were indeed replaced by a chelating ligand, which however was 3-methyl-2-hydroxymethyl-pyridine (m2hmp) and not 2hmp (Fig. 5). The same result was obtained using either $CHCl_3$ or $CH_3NO_2$ solution of 2hmp (when pure 2hmp was used, the crystals were destroyed). However, 2hmp (non-methylated) guest molecules are found in the pores of the exchanged compound interacting through hydrogen bonds (~2.7 Å) with the m2hmp ligands (Fig. S12†). The methyl-analogue of 2hmp incorporated into the structure of **EuN-BDC** cannot be an impurity in the 2hmp reagent used (since the $^1H$ NMR spectrum of the 2hmp reagent showed no presence of such a methyl-substituted compound), but is rather formed *in situ* and then inserted as a chelating ligand into **EuN-BDC**. Interestingly, a search in the Cambridge Crystallographic Database revealed that 3-methyl-2-hydroxymethyl-pyridine has not appeared in any crystal structure. The investigation of the formation of m2hmp in the presence of **EuN-BDC** will be a subject of future studies.

We could also isolate the exchanged analogue of **EuN-BDC** with a combination of one Im and one atzH terminal ligands per $Eu^{3+}$ ion (Fig. 5). Interestingly, the incorporation of two different terminal ligands per $Eu^{3+}$ ion was not possible for **UCY-8**, which contains one of these molecules as a terminal ligand and the second one as guest (*vide supra*). Finally, we have attempted to insert $merpdH_2$ into the structure of **EuN-BDC**, but this was not feasible.

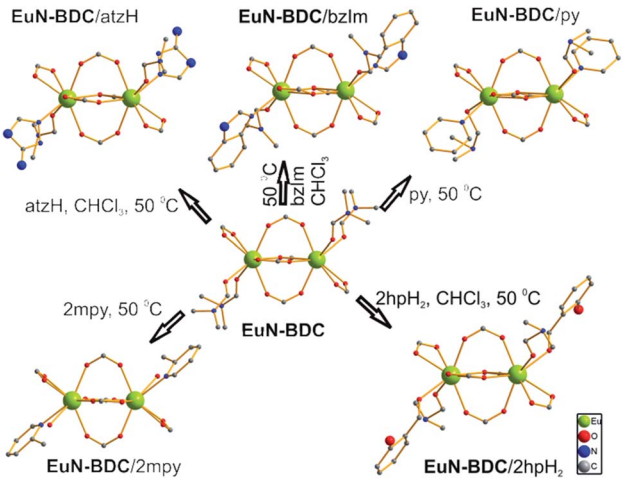


Fig. 4 SCSC transformations that resulted in the exchange of terminal solvent ligands of **EuN-BDC** by atzH, bzIm, py, 2mpy and $2hpH_2$.

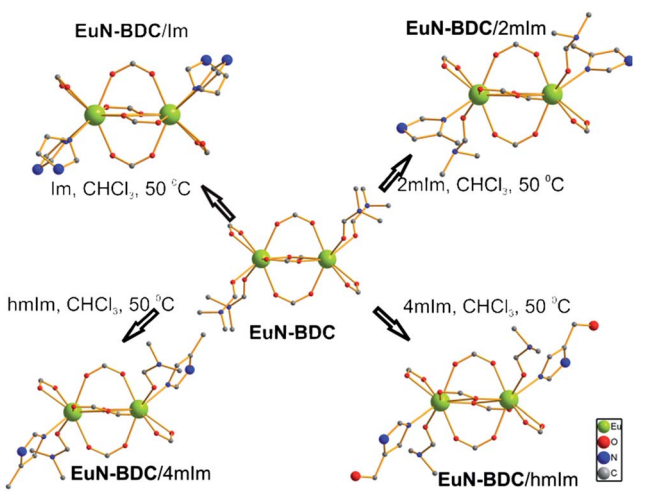


Fig. 3 SCSC transformations that resulted in the exchange of terminal solvent ligands of **EuN-BDC** by Im, 4(5)mIm, 2mIm and hmIm.

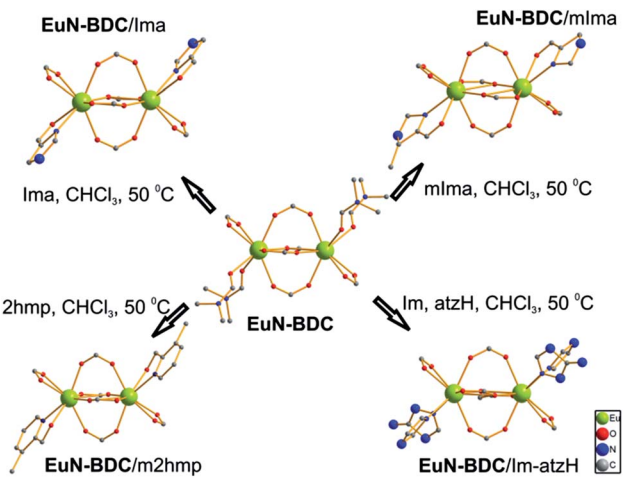


Fig. 5 SCSC transformations that resulted in the exchange of terminal solvent ligands of **EuN-BDC** by Ima, mIma, m2hmp and combination of Im/atzH.

### Modifications in the frameworks of UCY-8 and EuN-BDC upon insertion of organic molecules

The insertion of various organic molecules into **UCY-8** and **EuN-BDC** results not only in changes in the coordination environment of the $Eu^{3+}$ ions and/or type of guest molecules in the lattice, but also in significant modifications in some other structural characteristics of their frameworks. Thanks to these structural changes, **UCY-8** and **EuN-BDC** are capable of absorbing relatively bulky organic compounds, although both of these MOFs contain small pores and narrow channels with sizes 2–5 Å.[24,26] Specifically, the absorption capability of **UCY-8** is due to the breathing of its structure favoured by its significant flexibility, as also shown for other MOFs with flexible structures.[21,27] Examination of the unit cell and solvent accessible volumes[28] and the sizes of the pores and channels for the exchanged materials revealed significantly greater values than those of the pristine materials, indicating an expansion of the framework upon the diffusion of the organic molecules. The solvent accessible volumes for compounds **UCY-8**/py, **UCY-8**/2mpy and **UCY-8**/bzIm (40.5%, 43.2% and 49.4% respectively), which were calculated after excluding all guest molecules from the pores, are ~30–60% greater than the corresponding one for **UCY-8** (which is 31%). This shows the significant effect of the breathing phenomenon in the absorption capability of bulky organic molecules by **UCY-8**.

In the case of **EuN-BDC**, although the solvent accessible volumes of some exchanged MOFs, including **EuN-BDC**/2mIm, /4(5)-mIm, /hmIm, /2hpH$_2$ and /Im, are only slightly different (±~10%) from that of the pristine **EuN-BDC** MOF (20%), those of a few other exchanged analogues are significantly or even dramatically changed. Thus, the solvent accessible volumes of **EuN-BDC**/bzim (14%), **EuN-BDC**/atzH (29.1%), **EuN-BDC**/Ima (35.1%), **EuN-BDC**/mIma (45.4%), **EuN-BDC**/m2hmp (39.7%) and **EuN-BDC**/2mpy (41.5%) are 30–127% greater or smaller (in the case of **EuN-BDC**/bzim) than that of as-prepared **EuN-BDC**. Noticeably, the insertion into the structure of the **EuN-BDC** of the bulky bzIm and 2hpH$_2$ molecules reduced the solvent accessible volume, presumably because these ligands situated inside the cavities occupy more free space than the DMF terminal ligands of the pristine material. We have also calculated the theoretical nitrogen-accessible surface areas and maximum pore size/pore limiting diameter for the pristine **EuN-BDC** and **EuN-BDC**/mIma (that showed the highest solvent accessible volume) by using the program poreblazer_v3.0.[29] The results showed that the **EuN-BDC**/mIma has more than three times greater potential surface area (316 $m^2 g^{-1}$) than that of the pristine material (90 $m^2 g^{-1}$). In addition, the maximum pore size/pore limiting diameters of **EuN-BDC**/mIma (7.15/3.09 Å) are significantly larger compared to those of as-prepared **EuN-BDC** (5.31/1.88 Å). Therefore, SCSC coordinating solvent exchange may be a useful method to enhance the porosity of LnMOFs; studies towards this direction are in progress.

Apart from the solvent accessible volume and pore size diameters, there are also other significant modifications taking place in the frameworks of **EuN-BDC** and **UCY-8** upon the insertion of the various organic ligands. We will only describe the changes occurring in **EuN-BDC**, since they are rather unexpected for the theoretically rigid framework of this MOF. These modifications are apparent by overlaying the nets of **EuN-BDC** and those of *e.g.* **EuN-BDC**/2hmp, /mIma and /Ima, in which the dinuclear SBUs are shown as single octahedral nodes (Fig. 6). It can be seen that the nets of **EuN-BDC**/2hmp, /mIma and /Ima have substantially different orientations from that of pristine **EuN-BDC**. Although the node···node distances (11.2–14.6 Å) are similar for these nets, there are significant differences concerning the angles among the nodes (**EuN-BDC**: 61.2°, 80.4° and 99.7°; **EuN-BDC**/m2hmp: 110.6°, 54.7° and 98.7°; **EuN-BDC**/Ima: 50.79°, 84.49° and 72.72°; **EuN-BDC**/mIma: 72.3°, 63.7° and 88.9°).

It is remarkable that **EuN-BDC** showed very similar capability to **UCY-8** to exchange its coordinating solvent molecules with various organic ligands, taking into account that **EuN-BDC** contains small pores (2–5 Å) and theoretically has no structural flexibility (in contrast to **UCY-8**) that could help the diffusion of the organic ligands due to the breathing phenomenon. However, as revealed above by the comparison of the structural characteristics of pristine **EuN-BDC** and its exchanged analogues, it is apparent that there are significant structural changes taking place upon the insertion of some organic ligands into **EuN-BDC**, which are reminiscent of a behavior of a flexible rather than a rigid structure.

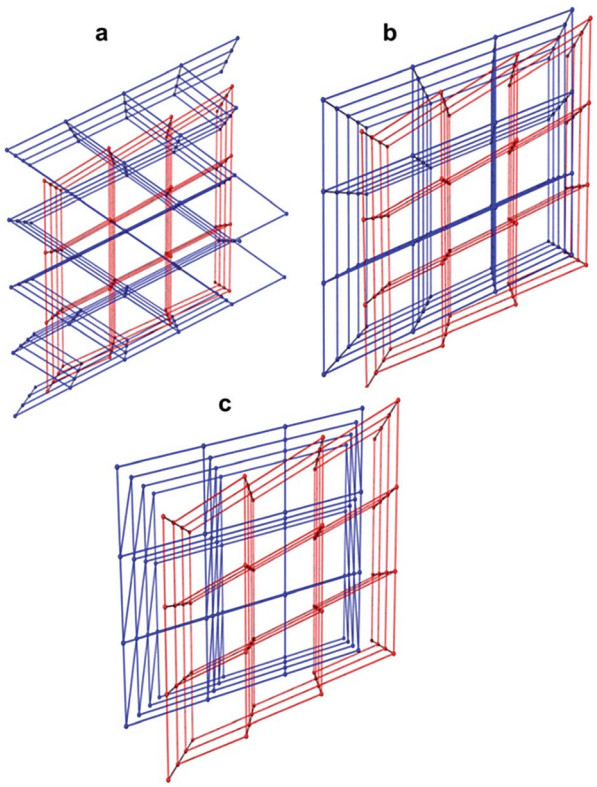


Fig. 6 Overlay of the net of EuN-BDC (red) with those of (a) EuN-BDC/Ima, (b) EuN-BDC/mIma and (c) EuN-BDC/m2hmp. In these nets, plotted using the X-SEED software,[30] each octahedral node represents a dinuclear SBU.

### Photophysical properties

The photophysical properties of the $Eu^{3+}$ MOFs were studied at room temperature in the solid state (microcrystalline powders) by steady state and time resolved luminescence spectroscopy. The $Gd^{3+}$ analogues were also studied as controls as the high energy of $Gd^{3+}$ excited states precludes ligand to metal energy transfer.

The solid state photoemission spectrum of **Eu-NBDC** (Fig. 7), upon excitation at 370 nm, in agreement with the findings of Reedijk *et al.*,[24] shows the characteristic sharp peaks due to luminescence originating from the $^5D_0 \rightarrow {}^7F_J$ transitions of the $Eu^{3+}$ ion at 595 nm ($J = 1$), 618 nm ($J = 2$), 653 nm ($J = 3$) and 700 nm ($J = 4$). The time resolved luminescence spectrum of **EuN-BDC** clearly shows a monoexponential decay of emission intensity corresponding to a lifetime of 260 ± 12 μs (Fig. S13†). This is consistent with the findings from the structural characterization of **EuN-BDC**, which show a single $Eu^{3+}$ site. The energies of the N-BDC $S_1$ and $T_1$ excited states are estimated from the onsets of ligand fluorescence and phosphorescence in **GdN-BDC** at *ca.* 24 100 $cm^{-1}$ and *ca.* 19 700 $cm^{-1}$ respectively (Fig. S14†). In principle both of these states may transfer energy to the lower-lying $^5D_0$ (17 500 $cm^{-1}$) excited state of the $Eu^{3+}$ ion. The fact that no residual ligand fluorescence and phosphorescence (even after application of a 40 μs time delay) could be detected in the emission spectrum of **EuN-BDC** shows that, efficient ligand to metal energy transfer takes place possibly from both the N-BDC $S_1$ and $T_1$ excited states. The close proximity between the energy donor and the acceptor in **Eu-NBDC** (the average distance between the center of the aromatic ring and the $Eu^{3+}$ ion is 5.65 Å) favors efficient sensitization of the $Eu^{3+}$ luminescence by the antenna effect as was observed in various $Eu^{3+}$ coordination polymers.[22a–c,31]

In the case of **UCY-8**, excitation at 265 nm (Fig. 8) gives rise to weak $Eu^{3+}$ emission at 595, 620, 654 and 701 nm ($Eu^{3+}$ $^5D_0 \rightarrow {}^7F_J$, $J = 1$, $J = 2$, $J = 3$ and $J = 4$ transitions respectively). The time resolved luminescence decay of **UCY-8** fits to a short lifetime of 18 ± 4 μs. When **UCY-8** is excited at 435 nm, the emission spectrum is dominated by a broad signal with a maximum at *ca.* 550 nm (Fig. 8, inset). **UCY-9** (the $Gd^{3+}$ analogue of **UCY-8**) shows a weak emission tail which levels off at *ca.* 750 nm upon excitation at 265 nm (Fig. S15†). Excitation of **UCY-9** at 435 nm gives rise to a weak and broad emission with a maximum at *ca.* 608 nm. The combined luminescence results from **UCY-8** and **UCY-9** suggest that the $CIP^{3-}$ ligand sensitizes $Eu^{3+}$ luminescence primarily through its higher excited states. However, the presence of low-lying excited states in $CIP^{3-}$ may lead to strong quenching of the $Eu^{3+}$ emission by thermal back energy transfer.[32] Moreover, the flexibility of the $CIP^{3-}$ ligand and the coordinated water molecule in **UCY-8** may provide additional non-radiative deactivation pathways through coupling of the $Eu^{3+}$ excited states to matrix vibrations.[33]

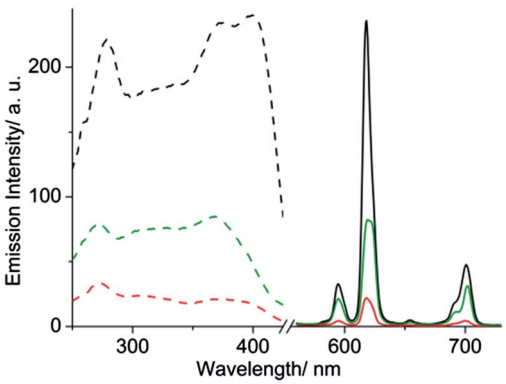


Fig. 7 Corrected solid state emission (solid lines) and excitation (dashed lines) spectra of EuN-BDC (red), EuN-BDC/Im (green) and EuN-BDC/m2hmp (black).

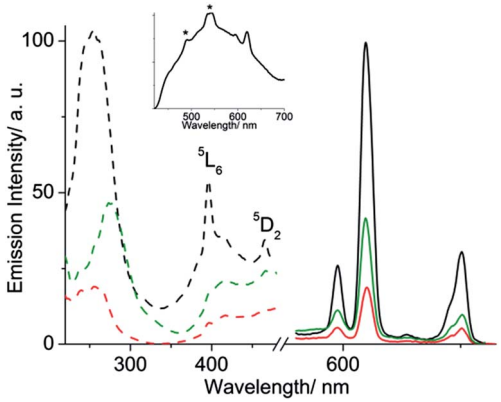


Fig. 8 Corrected solid state emission (solid lines) and excitation (dashed lines) spectra of UCY-8 (red), UCY-8/py (green) and UCY-8/4(5)mIm (black). Inset: the emission spectrum of UCY-8 exciting at 435 nm; (*) denotes instrument artifacts.

The solid state emission spectra of the **EuN-BDC** and **UCY-8** exchanged products containing various ancillary ligands (excitation at 370 and 265 nm respectively) show similar spectral features to those of the pristine compounds, however with significantly different intensities. In particular, the various exchange products of **EuN-BDC** generally show a substantial increase in luminescence intensity when compared to the pristine compound (Fig. 7). Especially, in the **EuN-BDC**/m2hmp exchange product the integrated intensity of the $Eu^{3+}$ $^5D_0 \rightarrow {}^7F_2$ transition increases by a factor of 10 when compared to that of the pristine compound, a difference that can clearly be seen by the naked eye (Fig. 9). The low energy part of the excitation spectrum of **EuN-BDC**/m2hmp shows two signals at *ca.* 373 and 400 nm. By comparison with the excitation spectrum of the pristine compound (Fig. 7), we assign the peak at 400 nm to the m2hmp ligand. This shows that the observed increase of emission intensity in **EuN-BDC**/m2hmp is partly the result of the presence of an additional strongly absorbing ligand which can also transfer excitation energy to $Eu^{3+}$.

On the basis of eqn (1),[34] we may estimate the emission quantum yield value of the $Eu^{3+}$ ion, $\Phi_{Eu}$, in the **UCY-8** and **EuN-BDC** derivatives by using the measured emission lifetime values, $\tau_{obs}$, of the solid samples and the radiative lifetime, $\tau_R$, of $Eu^{3+}$.

$$\Phi_{Eu} = \frac{\tau_{obs}}{\tau_R} \quad (1)$$

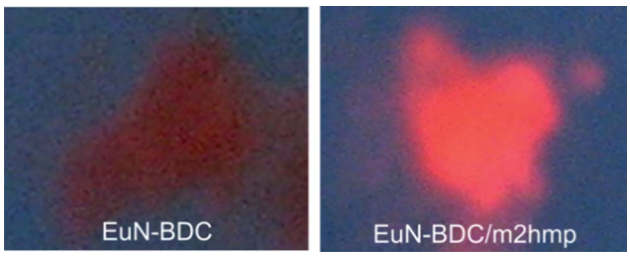


Fig. 9 Observed emission from crystals of **EuN-BDC** and **EuN-BDC**/m2hmp crushed on a filter paper and irradiated by a standard laboratory UV lamp ($\lambda_{exc}$ = 365 nm).

The radiative lifetime of $Eu^{3+}$ can be calculated using eqn (2)[34] where $A_{MD,0}$ is the probability for spontaneous emission for the $^5D_0 \rightarrow {}^7F_1$ transition *in vacuo* (14.65 $s^{-1}$), $I_{tot}/I_{MD}$ is the ratio of the total integrated intensity of the corrected $Eu^{3+}$ emission spectrum to the integrated intensity of the magnetic dipole $^5D_0 \rightarrow {}^7F_1$ transition and $n$ is the refractive index (1.5 for solid state metal–organic complexes).[35]

$$\frac{1}{\tau_R} = A_{MD,0} n^3 \frac{I_{tot}}{I_{MD}} \quad (2)$$

The emission lifetimes along with calculated $\tau_R$ and $\Phi_{Eu}$ values for the **EuN-BDC** and the **UCY-8** exchange products are summarized in Table 1. In the case of the **Eu-NBDC** series, the exchanged products show similar or significantly higher $\Phi_{Eu}$ values in comparison to the pristine compound. The adducts of **EuN-BDC** with 4(5)mIm, m2hmp and Im showed the most pronounced increase (by a factor of ~2) in the emission lifetime (495 ± 15, 530 ± 15 and 550 ± 27 μs respectively) compared to the pristine compound (260 ± 12). This corresponds to an increase in $\Phi_{Eu}$ from 15.1% in **EuN-BDC** to 24.6%, 24.1% and 31.6% in the **EuN-BDC**/4(5)mIm, **EuN-BDC**/Im and **EuN-BDC**/m2hmp exchanged products respectively.

Table 1 Luminescence data of the pristine **EuN-BDC** and **UCY-8** MOFs and selected exchanged analogues

| Compound | $\lambda_{exc}$/nm | $\tau_{obs}$/μs | $\tau_R$[a,b]/μs | $\Phi_{Eu}$[a,c] (%) |
|---|---|---|---|---|
| **EuN-BDC** | 370 | 260 ± 12 | 1721 | 15.1 |
| /Ima | 370 | 180 ± 12 | 1395 | 12.9 |
| /mIma | 370 | 230 ± 12 | 1528 | 15.0 |
| /2mIm | 370 | 300 ± 15 | 1817 | 16.5 |
| /hmIm | 370 | 310 ± 10 | 1717 | 18.1 |
| /4(5)mIm | 370 | 495 ± 15 | 2014 | 24.6 |
| /Im | 370 | 550 ± 27 | 2280 | 24.1 |
| /m2hmp | 370 | 530 ± 15 | 1676 | 31.6 |
| **UCY-8** | 265 | 18 ± 4 | 2017 | 0.9 |
| /2hmp | 265 | 68 ± 7 | 1753 | 3.9 |
| /mIma | 265 | 238 ± 15 | 2000 | 11.9 |
| /py | 265 | 118 ± 4 | 1926 | 6.1 |
| /2mIm | 265 | 122 ± 5 | 2064 | 5.9 |
| /4(5)mIm | 265 | 238 ± 15 | 2227 | 10.7 |
| /Im | 265 | 303 ± 22 | 2111 | 14.4 |

[a] Estimated error values: $\tau_R$ (±20%) and $\Phi_{Eu}$ (±20%). [b] Calculated using eqn (2) (see the main text). [c] Calculated using eqn (1) (see the main text).

**UCY-8** and its exchange products generally show significantly weaker $Eu^{3+}$ luminescence in comparison to that of the **EuN-BDC** series. However, among the **UCY-8** series we observe the most pronounced differences in $\tau_{obs}$ and $\Phi_{Eu}$ (Table 1). For example, in **UCY-8**, $\tau_{obs}$ and $\Phi_{Eu}$ are 18 ± 4 μs and 0.9% respectively, while in **UCY-8**/Im these values increase by a factor of ~16 to 303 μs and 14.4% respectively. The emission ($\lambda_{exc}$ = 265 nm) and excitation spectra (monitoring at the $^5D_0 \rightarrow {}^7F_1$ peak) of **UCY-8**, **UCY-8**/py and **UCY-8**/4(5)mIm, three representative members of the **UCY-8** series, are shown in Fig. 8. The excitation spectrum of **UCY-8** shows a weak and broad signal at *ca.* 255 nm attributed to π–π* transitions of the $CIP^{3-}$ ligand. In contrast, **UCY-8**/py and **UCY-8**/4(5)mIm show much more pronounced peaks at 275 and 255 nm respectively attributed to π–π* transitions of the py and 4(5)mIm ligands respectively. This shows that the additional aromatic ligands can sensitize $Eu^{3+}$ luminescence more effectively than the $CIP^{3-}$ ligand. However, in the low energy part of the excitation spectrum of **UCY-8**/4(5)mIm we observe two sharp signals of significant intensity at *ca.* 396 and 465 nm assigned to direct excitation of the $Eu^{3+}$ ion to the $^5L_6$ and $^5D_2$ states respectively. This indicates that, even though the presence of strongly absorbing imidazole ligands results in more effective sensitization of $Eu^{3+}$ luminescence, the overall antenna effect in the **UCY-8** series is still rather weak.

We therefore reach the conclusion that the enhancement of $Eu^{3+}$ luminescence in **UCY-8** and **EuN-BDC** upon exchange of the coordinating solvents with various ancillary ligands is mainly the result of (i) improved sensitization of $Eu^{3+}$ luminescence due to the presence of additional strongly absorbing aromatic ligands, (ii) increased protection of the metal from the quenching effect of mobile solvent molecules and (iii) the structural changes induced by the coordination of the new ligands possibly leading to less effective thermal deactivation due to lattice vibrations. One more important quenching mechanism present in both the **EuN-BDC** and **UCY-8** series is vibrationally assisted Eu–Eu energy transfer facilitated by the short intermetallic distances in these compounds. The shortest Eu–Eu distances in **EuN-BDC** and **UCY-8** are 4.07 and 4.02 Å respectively. These distances do not differ significantly in the exchange products (the shortest distances found are 3.96 and 3.98 Å for the **EuN-BDC**/m2hmp and **UCY-8**/2hmp respectively) and therefore the contribution of quenching by Eu–Eu energy transfer is expected to be similar within both series.

## Conclusions

In conclusion, we have performed a series of SCSC coordinating solvent exchange reactions for two types of $Eu^{3+}$ MOFs, the rigid **EuN-BDC** and flexible **UCY-8**. The compounds exhibit an exceptional capability to exchange their coordinating solvent molecules by imidazole and its derivatives, mercapto-propanediol, amino-triazole, chelating ligands and various bulky aromatic molecules. Thus, a large variety of free functional groups can be incorporated into the structure of these compounds including –NH–, –OH, $–NH_2$, –SH or combinations of them. Although the flexibility and breathing capacity of

 

**UCY-8** may facilitate the diffusion of bulky ligands into its small pores, it is really remarkable that **EuN-BDC** with no structural flexibility and narrow pores can also allow the incorporation of relatively large organic molecules into its structure. In fact, the insertion of some organic molecules into **EuN-BDC** substantially modifies its structure, thus revealing the presence of significant flexibility in a theoretically rigid framework. This may change the way we are thinking about the rigid LnMOFs that seem to be capable for the absorption of a variety of organic molecules including bulky ones even in the cases that these MOFs contain small pores and channels. Probably, the weak connection of the terminal neutral solvent molecules to $Ln^{3+}$ ions and their high mobility are the main driving forces for the capability of LnMOFs for SCSC coordinating solvent exchange that surpass various structural limitations (*e.g.* lack of structural flexibility, small pores, *etc.*). It is also interesting that the insertion of some organic ligands into **EuN-BDC** results in the significant expansion of its potentially void space indicating that Single Crystal Coordinating Solvent Exchange (SCCSE) can be also useful as a method to induce or enhance the porosity of LnMOFs. Overall these results for the SCSC transformations of **UCY-8** and **EuN-BDC** demonstrate that SCCSE may be applicable to a large variety of LnMOFs independently of their structural characteristics. In addition, investigation of the photophysical properties of **UCY-8** and **EuN-BDC** and their analogues revealed that the incorporation, *via* SCCSE, of ligands with capability to efficiently transfer energy to $Eu^{3+}$ resulted in a substantial enhancement of the emission lifetimes and quantum yields. Thus, the insertion *via* SCCSE of appropriate organic molecules into the structures of LnMOFs appears to be a rational and effective strategy for the development of superior photoluminescent materials. Finally, the SCSC coordinating solvent exchange studies on photoluminescent LnMOFs, as those presented here, may be a useful tool to unearth possible chemical sensing properties for these materials, taking into account the dramatic increase or decrease of the PL signal upon coordination of specific organic molecules to $Ln^{3+}$ ions.

## Acknowledgements

This work was supported by the Cyprus Research Promotion Foundation Grant ΔΙΔΑΚΤΩΡ/ΔΙΣΕΚ/0308/22 which is co-funded by the Republic of Cyprus and the European Regional Development Fund.

## Notes and references

1 (*a*) M. Eddaoudi, D. B. Moler, H. L. Li, B. L. Chen, T. M. Reineke, M. O'Keeffe and O. M. Yaghi, *Acc. Chem. Res.*, 2001, **34**, 319; (*b*) D. Bradshaw, J. B. Claridge, E. J. Cussen, T. J. Prior and M. J. Rosseinsky, *Acc. Chem. Res.*, 2005, **38**, 273.

2 G. Ferey, *Chem. Soc. Rev.*, 2008, **37**, 191.

3 N. L. Rosi, J. Eckert, M. Eddaoudi, D. T. Vodak, J. Kim, M. O'Keeffe and O. M. Yaghi, *Science*, 2003, **300**, 1127.

4 (*a*) S. T. Zheng, T. Wu, J. A. Zhang, M. Chow, R. A. Nieto, P. Y.Feng and X. H. Bu, *Angew. Chem., Int. Ed.*, 2010, **49**, 5362; (*b*) D. X. Xue, A. J. Cairns, Y. Belmabkhout, L. Wojtas, Y. Liu, M. H. Alkordi and M. Eddaoudi, *J. Am. Chem. Soc.*, 2013, **135**, 7660.

5 H. Hayashi, A. P. Cote, H. Furukawa, M. O'Keeffe and O. M. Yaghi, *Nat. Mater.*, 2007, **6**, 501.

6 R. E. Morris and P. S. Wheatley, *Angew. Chem., Int. Ed.*, 2008, **47**, 4966.

7 P. Dechambenoit and J. R. Long, *Chem. Soc. Rev.*, 2011, **40**, 3249.

8 B. L. Chen, L. B. Wang, F. Zapata, G. D. Qian and E. B. Lobkovsky, *J. Am. Chem. Soc.*, 2008, **130**, 6718.

9 P. Horcajada, C. Serre, G. Maurin, N. A. Ramsahye, F. Balas, M. Vallet-Regi, M. Sebban, F. Taulelle and G. Ferey, *J. Am. Chem. Soc.*, 2008, **130**, 6774.

10 L. Q. Ma, J. M. Falkowski, C. Abney and W. B. Lin, *Nat. Chem.*, 2010, **2**, 838.

11 K. K. Tanabe and S. M. Cohen, *Chem. Soc. Rev.*, 2011, **40**, 498.

12 S. Horike, S. Shimomura and S. Kitagawa, *Nat. Chem.*, 2009, **1**, 695.

13 (*a*) M. Kawano and M. Fujita, *Coord. Chem. Rev.*, 2007, **251**, 2592; (*b*) D. L. Reger, A. Debreczeni and M. D. Smith, *Inorg. Chem.*, 2011, **50**, 11754; (*c*) M.-S. Chen, M. Chen, S. Takamizawa, T.-A. Okamura, J. Fan and W.-Y. Sun, *Chem. Commun.*, 2011, **47**, 3787; (*d*) Z. Su, M. Chen, T.-A. Okamura, M. S. Chen, S.-S. Chen and W.-Y. Sun, *Inorg. Chem.*, 2011, **50**, 985.

14 Y. Inokuma, T. Arai and M. Fujita, *Nat. Chem.*, 2010, **2**, 780.

15 S. K. Ghosh, J. P. Zhang and S. Kitagawa, *Angew. Chem., Int. Ed.*, 2007, **46**, 7965.

16 L. R. Macgillivray, G. S. Papaefstathiou, T. Friscic, T. D. Hamilton, D. K. Bucar, Q. Chu, D. B. Varshney and I. G. Georgiev, *Acc. Chem. Res.*, 2008, **41**, 280.

17 T. Gadzikwa, O. K. Farha, K. L. Mulfort, J. T. Hupp and S. T. Nguyen, *Chem. Commun.*, 2009, 3720.

18 J. S. Costa, P. Gamez, C. A. Black, O. Roubeau, S. J. Teat and J. Reedijk, *Eur. J. Inorg. Chem.*, 2008, 1551.

19 H. J. Park, Y. E. Cheon and M. P. Suh, *Chem. – Eur. J.*, 2010, **16**, 11662.

20 O. Karagiaridi, W. Bury, A. A. Sarjeant, C. L. Stern, O. K. Farha and J. T. Hupp, *Chem. Sci.*, 2012, **3**, 3256.

21 M. J. Manos, E. J. Kyprianidou, G. S. Papaefstathiou and A. J. Tasiopoulos, *Inorg. Chem.*, 2012, **51**, 6308.

22 (*a*) J. Rocha, L. D. Carlos, F. A. A. Paza and D. Ananias, *Chem. Soc. Rev.*, 2011, **40**, 926; (*b*) Y. Cui, Y. Yanfeng, G. Qian and B. Chen, *Chem. Rev.*, 2012, **112**, 1126; (*c*) G. Katsagounos, E. Stathatos, N. B. Arabatzis, A. D. Keramidas and P. Lianos, *J. Lumin.*, 2011, **131**, 1776; (*d*) J. R. Choi, T. Tachikawa, M. Fujitsuka and T. Majima, *Langmuir*, 2010, **26**, 10437.

23 C. G. Efthymiou, E. J. Kyprianidou, C. J. Milios, M. J. Manos and A. J. Tasiopoulos, *J. Mater. Chem. A*, 2013, **1**, 5061.

24 C. A. Black, J. S. Costa, W. T. Fu, C. Massera, O. Roubeau, S. J. Teat, G. Aromi, P. Gamez and J. Reedijk, *Inorg. Chem.*, 2009, **48**, 1062.

25 C. K. Terajima, K. Yanagi, T. Kaziki, T. Kitazawa and M. Hasegawac, *Dalton Trans.*, 2011, **40**, 2249.

26 C. F. Macrae, P. R. Edgington, P. McCabe, E. Pidcock, G. P. Shields, R. Taylor, M. Towler and J. van De Streek, *J. Appl. Crystallogr.*, 2006, **39**, 453.
27 E. J. Kyprianidou, G. S. Papaefstathiou, M. J. Manos and A. J. Tasiopoulos, *CrystEngComm*, 2012, **14**, 8368.
28 A. L. Spek, *J. Appl. Crystallogr.*, 2003, **36**, 7.
29 L. Sarkisov and A. Harrison, *Mol. Simul.*, 2011, **37**, 1248.
30 L. J. Barbour, *J. Supramol. Chem.*, 2001, **1**, 189.
31 C. Daiguebonne, N. Kerbellec, O. Guillou, J. C. Bunzli, F. Gumy, L. Catala, T. Mallah, N. Audebrand, Y. Gerault, K. Bernot and G. Calvez, *Inorg. Chem.*, 2008, **47**, 3700.
32 L. Armelao, S. Quici, F. Barigelletti, G. Accorsi, G. Bottaro, M. Cavazzini and E. Tondello, *Coord. Chem. Rev.*, 2010, **254**, 487.
33 A. Beeby, I. M. Clarkson, R. S. Dickins, S. Faulkner, D. Parker, L. Royle, A. S. de Sousa, J. A. G. Williams and M. Woods, *J. Chem. Soc., Perkin Trans. 2*, 1999, 493.
34 M. H. V. Werts, R. T. F. Jukes and J. W. Verhoeven, *Phys. Chem. Chem. Phys.*, 2002, **4**, 1542.
35 N. M. Shavaleev, S. V. Eliseeva, R. Scopelliti and J. C. G. Bunzli, *Inorg. Chem.*, 2010, **49**, 3927.